nature astronomy

Article

https://doi.org/10.1038/s41550-022-01833-6

Direct detection of ultralight dark matter bound to the Sun with space quantum sensors

Received: 25 January 2022

Accepted: 14 October 2022

Published online: 5 December 2022

Check for updates

Yu-Dai Tsai[1,2,3] ✉, Joshua Eby[4] ✉ & Marianna S. Safronova[5,6] ✉

Recent advances in quantum sensors, including atomic clocks, enable searches for a broad range of dark matter candidates. The question of the dark matter distribution in the Solar system critically affects the reach of dark matter direct detection experiments. Partly motivated by the NASA Deep Space Atomic Clock and the Parker Solar Probe, we show that space quantum sensors present new opportunities for ultralight dark matter searches, especially for dark matter states bound to the Sun. We show that space quantum sensors can probe unexplored parameter space of ultralight dark matter, covering theoretical relaxion targets motivated by naturalness and Higgs mixing. If a two-clock system were able to make measurements on the interior of the solar system, it could probe this highly sensitive region directly and set very strong constraints on the existence of such a bound-state halo in our solar system. We present sensitivity projections for space-based probes of ultralight dark matter, which couples to electron, photon and gluon fields, based on current and future atomic, molecular and nuclear clocks.

In addition to explaining the dark matter (DM) of the universe, ultralight dark matter (ULDM) can be motivated by naturalness[1,2], string theory[3] and dark energy[4]. The 'fuzzy', wave-like nature of such particles can also affect structure formation[5]. An important probe of ULDM arises in precision tests using atomic clocks and other quantum technologies.

Space quantum technologies are known to have important practical applications, including the auto-navigation of spacecrafts[6], relativistic geodesy[7], linking Earth optical clocks[8], secure quantum communications[9] and others. The NASA Deep Space Atomic Clock (DSAC) mission has recently demonstrated a factor of 10 improvement over previous space-based clocks[10], and similar or better sensitivity has been achieved by the other atomic clocks in space[11]. We aim to demonstrate a new window of opportunity to study ULDM with such technologies, taking advantage of these and upcoming space missions to search for DM in environments that are drastically different from that of the Earth.

In this paper, we study an exciting new avenue of probing ULDM with future high-precision atomic, molecular and nuclear clocks in space; we sometimes refer to these as quantum clocks for simplicity. The oscillations of the ULDM field can induce a time-varying contribution to fundamental constants, including the electron mass and fine-structure constant (see, for example, refs. [12,13]). Exceptional enhancements of DM density that can be enabled by bound halos present an opportunity for direct DM detection with clocks[14].

We propose a clock-comparison satellite mission, tentatively dubbed *SpaceQ*, with two clocks onboard to the inner reaches of the solar system, to search for a DM halo bound to the Sun and also look for the spatial variation of the fundamental constants associated with a change in the gravitation potential. We show that the projected sensitivity of space-based clocks for detection of a Sun-bound DM halo exceeds the reach of Earth-based clocks by orders of magnitude. We consider

[1]Department of Physics and Astronomy, University of California, Irvine, CA, USA. [2]Fermi National Accelerator Laboratory (Fermilab), Batavia, IL, USA. [3]Kavli Institute for Cosmological Physics (KICP), University of Chicago, Chicago, IL, USA. [4]Kavli Institute for the Physics and Mathematics of the Universe (WPI), The University of Tokyo Institutes for Advanced Study, The University of Tokyo, Kashiwa, Japan. [5]Department of Physics and Astronomy, University of Delaware, Newark, DE, USA. [6]Joint Quantum Institute, National Institute of Standards and Technology and the University of Maryland, College Park, MD, USA. ✉e-mail: yudait1@uci.edu; yt444@cornell.edu; joshaeby@gmail.com; msafrono@udel.edu

both the projected bounds for the clocks that were already demonstrated, and the new nuclear and molecular clocks under development.

While a halo made of any scalar particle in the right mass range can be detected, an important target for this mission is the relaxion, a particle proposed to solve the hierarchy problem for the Higgs particle[1,15], which has the possibility to be DM as well[2]. We will show that our proposed mission can probe realistic model space for relaxions mixing with the Higgs boson (so-called Higgs portal models), and 'natural' theories of scalar DM more generally. Specifically, we focus on the 'naturalness' of the scalar field mass m_ϕ, which roughly corresponds to the condition that quantum corrections induced by scalar interactions do not exceed its bare mass; see, for example, ref. [16] and references therein. In fact, at present, to our knowledge, this is the only proposal capable of reaching these target sensitivities in our parameter space of interest (see also ref. [17] for probes in other parameter ranges).

In addition to searching for ULDM, we also briefly discuss other fundamental physics studies enabled by such clock-comparison experiments in space. A clock-comparison experiment in a variable-gravity environment can test the potential spatial variations of fundamental constants under the change in the gravitational potential[18]. Along these lines, we briefly show that our proposed mission can also improve the precision by two orders of magnitude for this measurement in comparison to similar tests on Earth or near-Earth orbits without any changes to the mission hardware.

Unless otherwise specified, we use the convention of natural units, where the reduced Planck's constant $\hbar$ and the speed of light c are equal to unity, in this work.

Quantum clock searches for ULDM

ULDM scalar field couplings to the Standard Model (SM) can induce oscillations of fundamental constants, including masses and couplings. Consider the following interaction Lagrangian for a DM scalar field ϕ:

$$\mathcal{L} \supset \kappa\phi\left(d_{m_e} m_e \bar{e}e + \frac{d_\alpha}{4} F_{\mu\nu}F^{\mu\nu} + \frac{d_g \beta_3}{2g_s} G^A_{\mu\nu} G^{A\mu\nu}\right), \quad (1)$$

where $d_{m_e,\alpha,g}$ are the dimensionless couplings of ULDM ϕ to electrons, photons and gluons, e is the electron field, $F^{\mu\nu}$ and $G^{A\mu\nu}$ are the electromagnetic and quantum chromodynamics (QCD) field strengths, respectively (labeled by the Lorentz indices μ, ν and the gauge index A), g_s and β_3 are the strong interaction coupling constant and beta function, respectively, and $\kappa = \sqrt{4\pi}/M_P$ with $M_P = 1.2 \times 10^{19}$ GeV. In a DM background field of amplitude $\phi = \phi_0$, the couplings in equation (1) induce modification of the electron mass m_e, fine-structure constant α and strong coupling $\alpha_s \equiv g_s^2/4\pi$, respectively. However, the fundamental oscillatory nature of the ULDM field implies that the contribution to these parameters is oscillatory as well, oscillating at the DM Compton frequency $\omega = m_\phi c^2/\hbar$.

Atomic physics experiments, including atomic clock-comparison tests, have shown great promise to probe these signals. The low fractional uncertainty in frequency that has been achieved corresponds to similar sensitivity to the oscillatory signals of the form

$$\mu(\phi) \simeq \mu_0\left(1 + d_{m_e}\kappa\phi\right), \quad \alpha(\phi) \simeq \alpha_0\left(1 - d_\alpha \kappa\phi\right)$$
$$\alpha_s(\phi) \simeq \alpha_{s,0}\left(1 - \frac{2d_g\beta_3}{g_s}\kappa\phi\right), \quad (2)$$

where $\mu = m_e/m_p$ is the electron–proton mass ratio, and the subscript '0' denotes the central (time-independent) value of μ, α and α_s. Variation of the strong coupling α_s gives rise to variation of the dimensionless ratio[19]

$$\left(\frac{m_q}{\Lambda_{QCD}}\right)(\phi) \simeq \left(\frac{m_q}{\Lambda_{QCD}}\right)_0 \left(1 - d_g\kappa\phi\right). \quad (3)$$

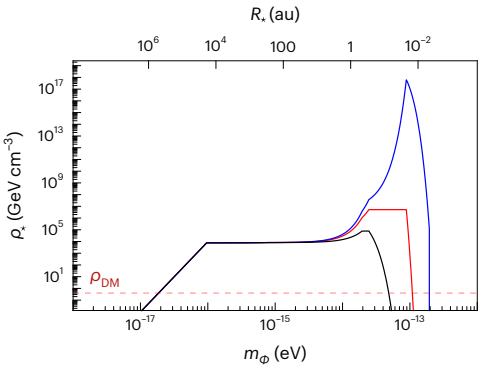

Fig. 1 | Maximum SH density. The allowed SH density $\rho_\star$, as a function of ULDM particle mass m_ϕ, at different probe radii: 1 au (radius of Earth's orbit, black line), 0.39 au (radius of Mercury's orbit, red line) and 0.1 au (blue line). The burgundy dashed line is the local density of virialized DM.

where Λ_{QCD} is the QCD scale and m_q is the averaged light quark mass. There are now many dedicated experiments searching for these types of signals (see, for example, refs. [13,20–25]).

Atomic clock accuracy has improved immensely over the past decade, and so too has their ability to test variation of fundamental constants; we review recent work in this field below. Other probes of ultralight scalar fields include equivalence principle (EP) and planetary precession tests, which do not need to assume anything about the DM density in the vicinity of the experiment, as they search for virtual exchange of ϕ particles that appear as a 'fifth force' not proportional to $1/r^2$ (see, for example, refs. [26–29]). Historically, EP tests have outperformed atomic physics probes across a wide range of ULDM mass parameters, with the exception of very light particles $m_\phi \lesssim 10^{-17}$ eV (ref. [24]), at least for generic couplings and under the usual assumption of $\rho_{DM} = 0.4$ GeV cm^{-3} for the local density of DM. On the other hand, atomic physics probes couple directly to the DM density and, therefore, allow for direct detection. Furthermore, such experiments have the ability to probe bound-state DM in our solar system, as we will explain below, and a space-based clock allows one to probe new parameter space as well. Future development of the nuclear clock, expected to be 10^4–10^5 times more sensitive to variations of α than all operating atomic clocks, will markedly increase the discovery reach of such experiments. In addition, the nuclear clock has strong sensitivity to m_q/Λ_{QCD}; see below for further details.

Solar system halos

The local DM density ρ_{DM} is a key parameter dictating experimental sensitivity; on the basis of halo modelling and (weak) local constraints (see below, as well as in Methods), its value is typically assumed to be $\rho_{DM} = 0.4$ GeV cm^{-3}. For ultralight particles, the field oscillates coherently on a timescale dictated by the virial velocity $v_{DM} \simeq 10^{-3}c$, given by $\tau_{coh} \approx 2\pi(m_\phi v_{DM}^2/\hbar c^2)^{-1} \simeq 2\pi \times 10^6 \hbar/m_\phi$ However, the possibility that a large density of such fields could become bound to objects in the solar system has been considered, which would give rise to unique signals and strongly modified values for the local DM density and timescale of coherent DM oscillations[14]. Here we focus on the specific case of a bound ULDM halo around the Sun, known as a solar halo (SH).

There are intriguing hints that some density of ULDM would become bound to the Sun. One piece of suggestive evidence arises in numerical simulations of galaxy formation in ULDM with $m_\phi \approx 10^{-22}$ eV, which have recently included the presence of baryons[30]. The simulation suggests that the same relaxation processes that form boson stars in the DM-only case can instead form a halo-like configuration, akin to a gravitational atom (analogous to a hydrogen atom ground state with a gravitational potential), in the presence of a baryonic potential. If this holds also at larger m_ϕ, as we will consider below, it implies a plausible

https://doi.org/10.1038/s41550-022-01833-6

formation mechanism for ULDM to become bound to the Sun. It has also been suggested that a SH could form from adiabatic contraction during star formation[31]. In this work, we analyse the consequences of the existence of a SH on atomic clock searches for ULDM, with a focus on possibilities for future missions in space; previous work has focused instead on terrestrial searches (for example, ref. [14]).

A SH can be thought of as similar to a boson star[32], but supported by the external gravitational force of the host body (the Sun) rather than self-gravity. The profile of the SH density function is exponential, essentially constituting a gravitational atom (analogous to the ground state of hydrogen) with radius of order[14]

$$R_\star \simeq \frac{M_P^2}{M_{\rm ext}\, m_\phi^2}, \tag{4}$$

where $M_{\rm ext}$ is the mass of the external host body (here, $M_{\rm ext} = M_\odot$); note that $R_\star$ is independent of the total mass in the halo $M_\star$. For ULDM masses of m_ϕ of a few 10^{-14} eV, the radius of a SH is roughly 1 au (the average orbital radius of the Earth) and $R_\star$ grows as $\propto m_\phi^{-2}$ as m_ϕ mass decreases. Therefore, terrestrial atomic probes are sensitive only to a lower mass range fixed by the requirement that $R_\star \gtrsim 1$ au.

Note that a bound halo around the Earth would modify signals in the higher mass range 10^{-12} eV $\lesssim m_\phi \lesssim 10^{-7}$ eV; we discuss the resulting effects on atomic clocks in orbit around the Earth in Supplementary Information.

Space-based atomic clocks are notably different from terrestrial ones regarding sensitivity to ULDM probes. First, a space clock would provide a new method to probe a SH at larger m_ϕ, when the radius of the SH in equation (4) is smaller than 1 au. Second, and perhaps more strikingly, the constraints on an SH with a small radius are very weak; if an atomic clock were able to make measurements on the interior region of the solar system, it could probe this highly sensitive range directly and set strong constraints on the existence of such a halo in our solar system. Current constraints on a SH in our solar system arise from measurements of solar system ephemerides, especially from Mercury, Mars and Saturn, which are known with high precision[33]. The resulting maximum mass of a SH, following ref. [14], is of order $10^{-12} M_\odot$ at $m_\phi \simeq 10^{-14}$ eV and weaker elsewhere; in what follows, we use the full range of gravitational constraints and we always enforce that $M_\star < M_\odot/2$ as a naive requirement on the total mass in our solar system. The maximum SH density at different distances in the solar system is illustrated in Fig. 1.

We also note that the effective coherence time of the oscillations of the bound ULDM field $\tau_\star$ is generically larger than that of the virialized DM scenario[14], where $\tau_{\rm DM} \simeq 10^6/m_\phi$. In a narrow range around $m_\phi \simeq 10^{-13}$ eV, however, $\tau_\star < \tau_{\rm DM}$ by a modest factor (not greater than 5), possibly reducing the sensitivity reach of atomic clock probes by as much as an order of magnitude; we discuss this further in Methods.

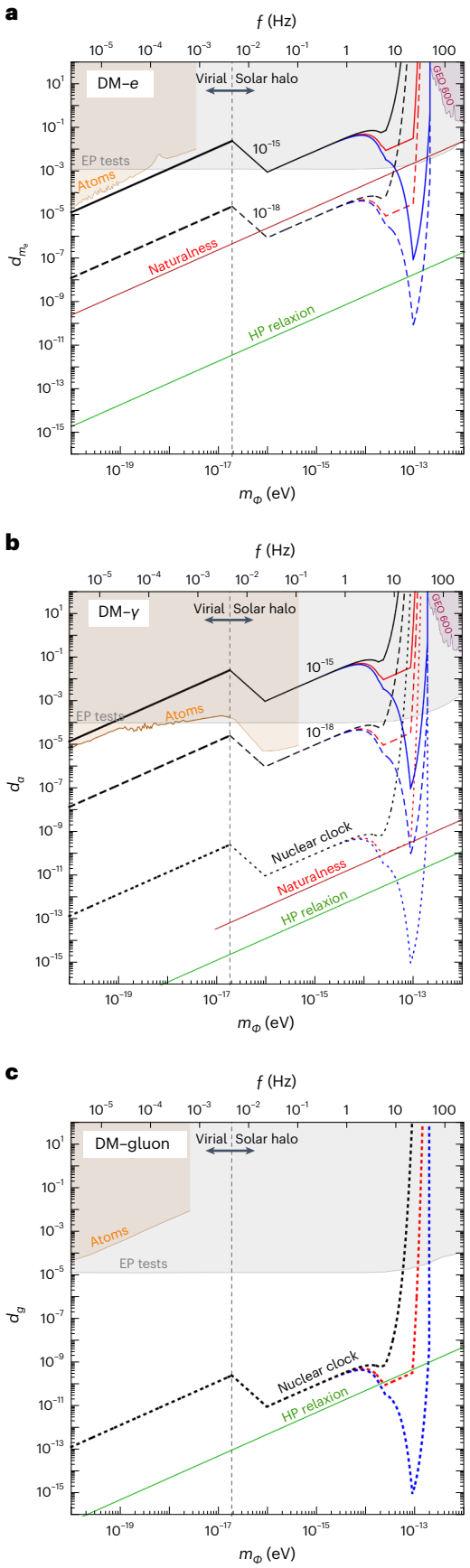

Fig. 2 | Sensitivity estimate for space quantum clocks. Estimated sensitivity reaches for ULDM, coupled via equation (1), assuming bound states around the Sun with the density given in Fig. 1 on the right of the vertical dashed line, or the virial DM density $\rho_{\rm DM}$ to the left of this line. The blue, red and black denote sensitivity for probes at the distance of 0.1 au, probes at the orbit of Mercury and for terrestrial clocks, respectively; note that distances of $r < 0.1$ au have been reached by the NASA PSP mission, reaching 0.06 u on its most recent perihelion and aiming for 0.045 au at the closest approach[40]. **a**–**c**, Projected bounds for the variations of the electron–proton mass ratio μ (**a**), fine-structure constant α (**b**) and ratio $m_q/\Lambda_{\rm QCD}$ (**c**). The thick and dashed lines correspond to assumed experimental sensitivities of 10^{-15} and 10^{-18}, respectively, for **a** and **b**. The dotted lines in **b** and **c** represent the projection for a clock-comparison experiment at the 10^{-19} level involving a nuclear clock; a 10^4 sensitivity factor is assumed for a nuclear clock (see Methods and, for example, ref. [56]). The grey, orange and purple shaded regions denote the current constraint from EP tests[26–28], atomic physics probes of the local DM density $\rho_{\rm DM}$ (refs. [13,20,21,24]) and the GEO 600 interferometer[67], respectively; the diagonal burgundy and green solid lines denote motivated theory targets[15], for scalar field naturalness and Higgs portal (HP) couplings mentioned in the introduction, respectively.

https://doi.org/10.1038/s41550-022-01833-6

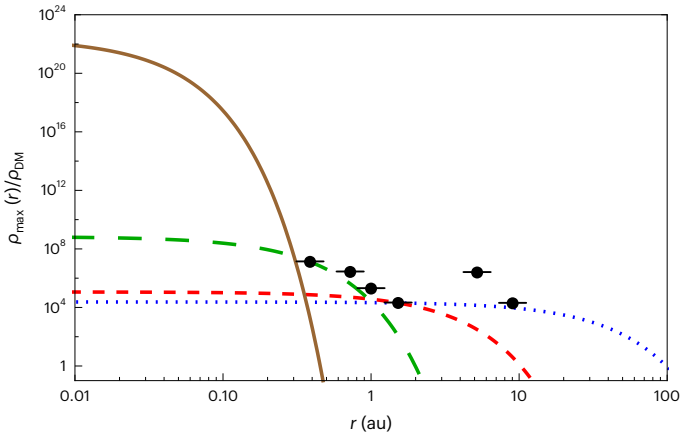

Fig. 3 | Maximum SH density as function of distance. The maximum allowed density $\rho_{max}(r)$ relative to background DM density ρ_{DM} as a function of distance from the Sun r. The blue dotted, red dashed, green long-dashed and brown solid lines correspond to ULDM particle masses of $m_\phi = 3\times10^{-15}$ eV, 10^{-14} eV, 3×10^{-14} eV and 10^{-13} eV, respectively. The black points denote the constraints at the orbital radii of Mercury, Venus, Earth, Mars, Jupiter and Saturn (left to right in the figure)[33].

Atomic, molecular and nuclear clocks

To detect ULDM with high-precision clocks, one measures a frequency ratio of two clocks with different sensitivities to the variation of fundamental constants over a period of time[12]. The discrete Fourier transform of the resulting time series then allows the extraction of a peak at the DM Compton frequency, with an asymmetric lineshape[12]. The lack of such a signal allows one to establish bounds on the DM parameter space. It is also possible to carry out such a measurement with a single clock by comparing the frequency of atoms to the frequency of the local oscillator (that is, cavity)[34].

The present proposal calls for a two-clock or clock–cavity setup onboard a satellite. It does not require a comparison to Earth-bound clocks. There are several factors one has to consider and questions to answer when selecting clocks for a proposed mission: (1) which variations of fundamental constants do we want to probe and what are the corresponding sensitivity factors; (2) what are the clock stabilities and systematic uncertainties; and (3) the difficulty of making these clocks space-ready. We discuss these in detail in Methods.

In addition to currently operating atomic clocks[35], a number of new clocks are being developed[36], based on molecules and molecular ions[37], highly charged ions (HCIs)[38] and the ^{229}Th nucleus[39].

Sensitivity reach

We estimate the sensitivity of a space-based quantum clock to the oscillation of fundamental constants, originating in ULDM fields of mass m_ϕ bound to the Sun. In Fig. 2, we estimate the reach for oscillations of μ, α and m_q/Λ_{QCD} (through the couplings in equation (1)) in Fig. 2a, b and c, respectively. As input, we take the possible distances from the Sun of $r = 1$ au (terrestrial searches), $r = 0.39$ au (the orbital radius of Mercury) and the far-future potential for a probe at $r = 0.1$ au; this latter distance is used as a demonstration, and we note that the NASA Parker Solar Probe (PSP) has already reached this inner orbit and has in fact been even nearer to the Sun, reaching 0.06 au on its most recent perihelion and is aiming for 0.045 au at the closest approach[40]. The PSP instruments are designed to study particles and electromagnetic fields for its scientific missions. Operating atomic clocks in an extreme environment within the Mercury orbits is a subject for future investigation. We note that the Mercury Laser Altimeter Instrument demonstrated a successful laser operation for the MESSENGER mission[41].

We observe that, for probes in this inner region of the solar system, there is a clear 'peak' in the sensitivity reach around $m_\phi \simeq 10^{-13}$ eV, which roughly corresponds to the point where $R_\star \simeq 0.1$ au; at larger m_ϕ, the exponential cutoff of the SH density function rapidly diminishes the sensitivity (see equation (6)).

In Fig. 2a,b, we assume a space-based clock-comparison with accuracy at the level of 10^{-15} (thick lines) or 10^{-18} (dashed lines); the former represents just below an order of magnitude improvement compared to what has already been demonstrated in DSAC[10], and the latter is already achievable for the variation of α in terrestrial optical clock-comparison experiments (see Methods and, for example, refs. [42–44]). In Fig. 2a for the 10^{-18} limit, one of the clocks has to be based on the molecular transition to provide sensitivity to the variation of μ; see refs. [36,45] for the projected sensitivities. We observe that even a sensitivity of 10^{-15} to these oscillations allows one to probe an interesting model space in a narrow range around $m_\phi \approx 10^{-13}$ eV, and space clocks at the 10^{-18} level could exceed EP probes over a wide range 3×10^{-17} eV $\lesssim m_\phi \lesssim 2\times10^{-13}$ eV, for a bound SH.

In Fig. 2b,c, we include a projection for a clock-comparison experiment at the 10^{-19} level involving a nuclear clock (dotted lines), assuming $\Delta K \simeq 10^4$, which is in line with future projections outlined above.

To estimate the sensitivity, we assume a bound SH in the parameter range $m_\phi \gtrsim 2\times10^{-17}$ eV, as this is where the bound density can exceed the virial DM component $\rho_\star > \rho_{DM}$ (Fig. 1); for smaller m_ϕ the virial component dominates the density and therefore provides the best sensitivity reach. When appropriate, we rescale the existing experimental constraint from atomic physics searches (labelled 'Atoms' in Fig. 2) by the SH density as well. For the SH density, we fix the total bound scalar mass $M_\star$ by the maximal bound-state mass allowed by current constraints, although our projection can be easily rescaled to less optimistic input values using $d^{limit} \propto \phi^{-1} \propto \rho^{-1/2} \propto M_\star^{-1/2}$. As a result, the shape of the sensitivity curves in Fig. 2 maps closely to the current upper limit on bound SH density at the relevant radii in the solar system; see Fig. 1 and Supplementary Information for details, and in particular Figs. 3 and 4 for the allowed range of densities over a wider range of distances from the Sun and particle masses. Also see Fig. 5 for a more complete description of the coherence time of the field, which is relevant to the sensitivity.

The diagonal burgundy and green lines represent model targets: a naive naturalness requirement on the coupling with cutoff scale $\Lambda = 3$ TeV and the boundary of physically realized Higgs portal models utilizing a relaxion, respectively[15]. We observe that the relaxion benchmark is reachable by future space-based clocks for any of the three couplings we consider in this work, whereas terrestrial clocks may require much greater increases in sensitivity reach to achieve the same for a certain mass range. Finally, note that, in some classes of models, constraints from EP tests are weaker than illustrated in Fig. 2, implying the advantage of direct searches in such models[25].

A space probe with a nuclear clock would allow one to probe a vastly larger parameter space, reaching for the first time physically motivated model space for Higgs-relaxion mixing (below the green line) for both photon and QCD couplings.

Spatial variation of fundamental constants

With our proposal of a space mission with a clock-comparison experiment in an inner solar orbit, one can also test the variations of fundamental constants due to the change in the gravitational potential during the satellite's transit to its orbit. Such new physics is usually parameterized as[37,46]

$$k_X \equiv c^2 \frac{\delta X}{X\,\delta U}. \tag{5}$$

We quantify the change in gravitational potential as δU between the positions of two clock measurements, and $X = \alpha, \mu$ or m_q/Λ_{QCD}. There are essentially differential redshift experiments.

https://doi.org/10.1038/s41550-022-01833-6

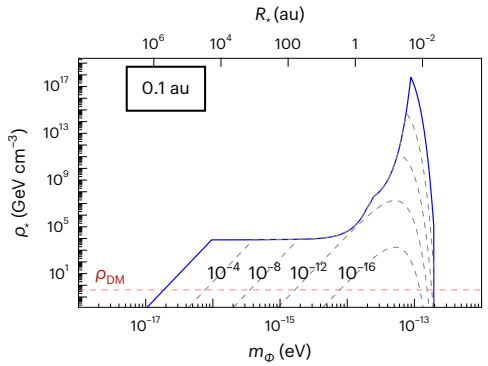

Fig. 4 | Maximum SH density at 0.1 au with contours. The allowed SH density $\rho_\star$ as a function of ULDM particle mass m_ϕ, at 0.1 au (blue line), along with contours of fixed $M_\star/M_\odot$ as labelled.

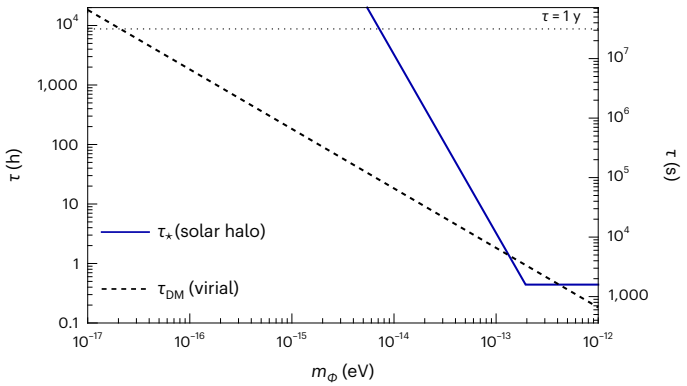

Fig. 5 | SH coherence time. The coherence timescale for a SH (blue) and for virialized DM (black dashed), as a function of ULDM particle mass m_ϕ.

Monitoring the ratio of clocks as the satellite moves deeper in the solar system can set strong constraints on the parameters k_X, as $(k_X)_{exp} = (\delta X/X)_{exp} c^2/\delta U$.

Previous studies make use of the seasonal variation in Earth's orbital distance to the Sun, which gives rise to a difference of $\delta U/c^2 \simeq 3.3 \times 10^{-10}$, which is used to constraint k_X(ref. [46]). For a probe at 0.1 au, as we have considered in this proposal, one can expect a change of the potential in comparison with 1 au of $\delta U/c^2 \approx 9 \times 10^{-8}$, which is about 300 times larger than that of the Earth's annual modulation. If the same uncertainty on measuring $\delta X/X$ can be reached in space as on Earth, one can therefore achieve constraints on k_X that are a factor of ~300 stronger, barring systematic uncertainties due to the space mission.

Probing the spatial variation of fundamental constants can be done with the space mission proposed here without any hardware modifications; it does not require an optical time transfer link between the satellite and Earth-based clocks. Such probe uses the variance of the gravitational potential during the mission flight towards the near Sun approach. The frequency ratio of clocks will be recorded while the mission is still on near-Earth orbit, with a duration just long enough to achieve goal sensitivity. This value will be compared with the frequency ratio obtained as a part of the SH search near the Sun to provide dependence of the clock ratio frequency (and therefore fundamental constants) on the gravitational potential. Even better statistics can be achieved if such measurements are done periodically as the mission flies towards the Sun. The clock specifications for such a test are exactly the same, as the maximum sensitivity to the variation of fundamental constants is all that is required.

We note that the SpaceTime mission with three trapped ion microwave clocks based on mercury, cadmium and ytterbium ions, in the same environment on a spacecraft that approaches the Sun to within four solar radii, was proposed in ref. [18] to probe apparent spatial variations of the fundamental constants associated with a change in the gravitational potential. The idea of sending a 'destructive' space probe directed into the Sun with a clock onboard and clock-comparison link to Earth to constrain Yukawa-type interactions of scalar particles (with the Sun as the source body) was proposed in ref. [47].

Other applications and outlook

We present an opportunity to study ULDM in unexplored and theoretically motivated regions with atomic, molecular and nuclear clocks in space. Such clocks can probe a large parameter space for ULDM bound to the Sun, with the possibility in the near future of reaching well-motivated theory targets. Additionally, a clock in a near approach to the Sun can substantially improve limits on the spatial variation of fundamental constants.

Below, we briefly discuss some natural extensions of our ideas, as well as other well-motivated physics topics that space and quantum technologies can probe.

Space quantum clock networks

A network of clocks in space and on Earth can study many fundamental physics topics, including transient topological DM[48] and multimessenger signatures of exotic particles[49] (note that the methodology of ref. [49] was criticized in ref. [50]). In our consideration, if a signal were to be present, the comparison of ground- and space-based clocks could help to map the density of DM in the vicinity of Earth to further constrain the bound DM scenario. One could set up a network of atomic and nuclear clocks on Earth and in space for this purpose. A high-precision clock in space with an optical link to Earth will also enable us to compare optical clocks at any place on Earth, without the need for a fibre-link connection.

Screening

An additional motivation for a space-based atomic clock arises when the ULDM scalar field possesses quadratic couplings to SM fields. For example, in the presence of a coupling of the form $\mathcal{L} \supset g_2 \frac{\phi^2}{M_P^2} m_i \bar{\psi}_i \psi_i$

(where ψ_i are SM fields of mass m_i) with a positive coefficient, there is a screening of the field value in the vicinity of the Earth, owing to a backreaction of the large number density $\bar{\psi}\psi$ of, for example, electrons or neutrons in the Earth, rapidly reducing the sensitivity of terrestrial experiments[28]; the effect is even more severe for transients[50]. A space-based probe considered in this work would not be subject to this Earth screening effect. If the quadratic coupling has a negative sign, the effect is instead an antiscreening of the field[28].

Gravitational redshift

Our present proposal does not require an optical link to enable comparison of satellite and Earth-based clocks. If such a link can be achieved, one can also directly test general relativity and provide a direct bound on the anomalous gravitational redshift exceeding present bounds by orders of magnitude (see ref. [51] for the current status and dedicated space mission proposal). Precision orbit determination will also be required.

Methods

Properties of a bound SH

Under the usual assumptions, DM exists in a virialized configuration with a roughly constant density $\rho_{DM} = 0.4$ GeV cm^{-3} in our solar neighbourhood. The strongest local constraints arise from the orbital dynamics of planets in the solar system, that is, solar system ephemerides; observations constrain the density of DM at the orbital

radius of Mercury, Venus, Earth, Mars, Jupiter and Saturn at the level of $\rho \lesssim 10^3$–10^5 GeV cm^{-3} (ref. [33]), which are shown by the black dots in Fig. 3.

We have been considering the scenario in which ULDM fields become bound to objects in the solar system, in which case the density and coherence properties will be modified in ways that are relevant to experimental searches[14]. A bound SH is essentially similar to a gravitational atom, with the Sun playing the role of the nucleus; therefore, the SH density function can be approximated as an exponential,

$$\rho_\star(r) \simeq \rho_0 \exp\left(-2r/R_\star\right), \tag{6}$$

as long as $r \gg R_\star \gg R_\odot$, in precise analogy to the ground state of a hydrogen atom. As explained in the main text, the radius $R_\star$ is fully determined by its host mass $M_{\rm ext}$ (in the case under consideration, $M_{\rm ext} = M_\odot$) and the ULDM particle mass m_ϕ; see equation (4). Therefore, the density function $\rho(r)$ for a SH is fully calculable, given input values of scalar mass m_ϕ, radius r and overall density normalization ρ_0. For a density that saturates the limits of ref. [33], we show the resulting density function $\rho(r)$, relative to $\rho_{\rm DM}$, for a few relevant choices of m_ϕ, in Fig. 3.

Given the above discussion of SH properties, we can translate the constraints on the local DM density from ref. [33] into a constraint on $\rho_\star$ as a function of m_ϕ. This is what is shown in Fig. 1: we have illustrated the resulting limits on SH density $\rho_\star$ at a distance of 1 au from the Sun (relevant for Earth-based probes, black line), a distance of 0.39 au (average radius of Mercury's orbit, red line) and for a distance of 0.1 au (blue line). In Fig. 4, we illustrate the same maximum density at 0.1 au, but include contours to show the density for different choices of $M_\star/M_\odot$. Note that, for consistency, we enforce $M_\star < M_\odot/2$ over the full range of parameters. It is evident from the figure that the constraint on the local density of DM bound to the Sun becomes very weak when measured inside the orbit of Mercury. As the contours illustrate, we observe that even a very small bound mass, of order $10^{-16} M_\odot$, can give rise to a 10^4 increase in the density of DM at 0.1 au for $m_\phi \simeq 10^{-13}$ eV.

To estimate the experimental reach of an atomic clock to probe a SH, we saturate the constraint on SH density at a given radius r (Fig. 1). This translates into a field amplitude $\phi_\star = \sqrt{2\rho_\star}/m_\phi$ which we substitute in equation (2). Then, we fix a value for the fractional accuracy in the variation of the fundamental constants (for example, 10^{-15}) motivated by current and near-future experiments (see next section), and derive the resulting sensitivity reach using

$$d_{m_e}^{\rm limit} \simeq \frac{1}{\kappa \phi_\star(r)} \left(\frac{\delta\mu}{\mu}\right)_{\rm exp}, \tag{7}$$

$$d_{\alpha}^{\rm limit} \simeq \frac{1}{\kappa \phi_\star(r)} \left(\frac{\delta\alpha}{\alpha}\right)_{\rm exp}, \tag{8}$$

$$d_{g}^{\rm limit} \simeq \frac{1}{\kappa \phi_\star(r)} \left(\frac{\delta(m_q/\Lambda_{\rm QCD})}{(m_q/\Lambda_{\rm QCD})}\right)_{\rm exp}. \tag{9}$$

The results are indicated by the black, red and blue lines in Fig. 2, respectively.

The coherence timescale for ULDM oscillations is typically much longer in a SH than it would be for virial DM $\tau_{\rm DM}$. This is because the bound ULDM particles much be colder, that is have lower velocity dispersion, to remain bound to the Sun. The velocity dispersion $v_\star$, and therefore the coherence timescale $\tau_\star$, of a SH is essentially dictated by its radius $R_\star$ and particle mass m_ϕ via the relation[52]

$$\begin{aligned}\tau_\star &\simeq \left(m_\phi v_\star^2\right)^{-1} \simeq m_\phi R_\star^2 \\ &\simeq 10^3 \text{ sec} \times \begin{cases} 1, & m_\phi \gtrsim 2\times10^{-13} \text{ eV} \\ \left(\frac{2\times10^{-13}\text{eV}}{m_\phi}\right)^3, & m_\phi \lesssim 2\times10^{-13} \text{ eV}. \end{cases}\end{aligned} \tag{10}$$

The transition point indicates where $R_\star \simeq R_\odot$, although sensitivity to the SH is still possible at $r > R_\star$ owing to the exponential tail of the density function (Fig. 3). This relation is illustrated in Fig. 5. When $\tau_\star$ is much longer than the averaging period τ of an atomic clock DM search (see discussion around equation (12)), the full stability of the clock can be leveraged; on the other hand, when $\tau_\star < \tau$, the sensitivity to ULDM signals grows much more slowly, as $\tau^{1/4}$ rather than $\tau^{1/2}$. For searches that are shorter, say of order $\tau \simeq 1$ day, the resulting reduction in sensitivity is about one order of magnitude at worst, when $m_\phi \gtrsim 2\times10^{-13}$ eV.

Present and future quantum clocks

The dimensionless sensitivity factors K of a pair of clocks translate the fractional accuracy of the ratio of frequencies ν to the fractional accuracy in the variation of the fundamental constant. For example, for the fine-structure constant

$$\frac{\partial}{\partial t} \ln \frac{\nu_2}{\nu_1} = (K_2 - K_1) \frac{1}{\alpha} \frac{\partial \alpha}{\partial t}, \tag{11}$$

where indices 1 and 2 refer to clocks 1 and 2, respectively. If the frequency ratio is measured with relative 10^{-18} precision and $\Delta K \equiv K_2 - K_1 = 1$, then such an experiment will be able to measure the fractional change in α with 10^{-18} precision. If $\Delta K = 10^4$, then the 10^{-18} accuracy of the frequency ratio allows one to detect a change in α at the 10^{-22} level. The sensitivity factors K to α variation for all atomic clocks can be computed from first principles with high precision[53]. They tend to increase for atoms with heavy nuclei for states with similar electronic configurations. Specific details of the electronic structure can lead to substantially larger enhancement factors.

At present, all operating atomic clocks are either based on transitions between the hyperfine substates of the ground state of the atom (microwave clocks: H, DSAC Hg^+, Rb, Cs) or transitions between different electronic levels (optical clocks: Al^+, Ca^+, Sr, Sr^+, Yb, Yb^+ and others)[35]. The typical frequencies of the optical clock transitions are 0.4–1.1×10^{15} Hz, while the frequencies of the microwave clocks are several orders of magnitude smaller, being a few gigahertz. The optical clock frequency is only sensitive to the variation of α, with varying sensitivity factors K. Microwave clocks are sensitive to variation of α and the $\mu = m_e/m_p$ ratio (with a sensitivity factor of $K = 1$), and there is also a small sensitivity of microwave clocks to $m_q/\Lambda_{\rm QCD}$. The sensitivities to the variation of α of most currently operating optical clocks are small: $K(Al^+) = 0.01$, $K(Ca^+) = 0.1$, $K(Sr) = 0.06$, $K(Sr^+) = 0.4$, $K(Yb) = 0.3$, $K(Yb^+$ E2$) = 1$, with a notable exception of the Yb^+ clock based on the octuple transition with $K = -6$ (ref. [53]). For the microwave Cs clock, $K = 2.83$. The most recent limits on the slow drifts of α and μ are given in ref. [54]. Comparing any optical clock to a cavity gives $\Delta K = 1 + K_{\rm clock}$, where $K_{\rm clock}$ is given above.

A lattice clock based on the $4f^{14}6s6p\ ^3P_0$–$4f^{13}6s^25d\ J = 2$ transition in neutral Yb was proposed with $K = 15$ (ref. [55]). HCI clocks and a nuclear clock have much higher sensitivities to α, $K \approx 100$ for HCIs and $K = -(0.82 \pm 0.25)\times10^4$ (ref. [56]) for a nuclear clock, with the actual sensitivity to be determined with the aid of future measurements of nuclear properties. HCI clocks have to operate in a cryogenic 4 K environment, complicating space deployment. Nuclear clocks can be operated as a trapped ion or a solid-state clock[39]. A solid-state nuclear clock could be particularly attractive for a space mission. Molecular clocks provide sensitivity to m_e/m_p variation and a nuclear clock is highly sensitive to hadronic sector, with possible $K = 10^4$ sensitivity to the variation of $m_q/\Lambda_{\rm QCD}$ (ref. [57]).

There are two characteristics to consider when evaluating state-of-the-art clocks: stability and uncertainty[35]. Stability is the precision with which we can measure a quantity. It is usually determined as a function of averaging time, since noise is reduced through averaging for many noise processes, and the precision increases with repeated measurements. One can probe the resonance using the Ramsey method

of separated fields in the regime in which the stability is limited by fundamental quantum projection noise, which involves applying two π/2 laser pulses with a wait (free-precession) time in between and thereby creating a superposition of two clock states. In this case, a clock instability is limited by[35]

$$\sigma(\tau) \approx \frac{1}{2\pi\nu_0\sqrt{NT_m \min(\tau, \tau_\star)}}, \quad (12)$$

where ν_0 is the clock transition frequency, N is the number of atoms or ions used in a single measurement, $T_m \approx 2\pi\delta\nu$ is the maximum possible time of a single measurement cycle (that is, the free-precession time where $\delta\nu$ is the spectroscopic linewidth of the clock transition) and τ is the averaging period[35]. Generally, T_m is still limited by the clock laser coherence rather than the natural linewidth, which represents a fundamental limit. This formula demonstrates the advantages of optical clocks over microwave clocks owing to the five orders of magnitude increase in the clock transition frequency ν_0. We discuss present and near-future clock stabilities below.

The absolute uncertainty of an atomic clock describes how well we understand the physical processes that shift the measured frequency from its unperturbed natural value. Several optical clocks have reached uncertainty at the 10^{-18} level (see, for example, ref. [42]), while microwave clocks are at the 10^{-16} level[58], which is at the achievable technical limit. There is no apparent technical limit to the substantial further improvement of optical clocks. Portable high-precision optical clocks have also been demonstrated[59]. Molecular clocks are projected to reach 10^{-18} uncertainties[45]. HCI clocks and a nuclear clock are estimated to achieve 10^{-19} uncertainties[38].

We now consider all parameters in equation (12) in the context of DM detection. To achieve high precision, the atoms or ions that serve as the frequency standards have to be trapped, leading to important differences in atom and ion clock design due to different trapping technologies. Neutral atom clocks are sometimes referred to as 'lattice clocks', as atoms are held in optical lattices, that is, light potentials created by counterpropagating laser beams. While ion trap technology design is simpler than that of lattice clocks, all of the ion clocks are presently operating with a single ion, that is, $N = 1$, leading to lower stability compared to the optical lattice clocks that commonly have $N \approx 1{,}000$, but the development of multi-ion clocks is in progress[60].

However, there have been substantial recent advances in the stability of optical atomic clocks with demonstrated operation at the quantum projection noise (QPN) limit. The lattice Sr clock with 100,000 atoms demonstrated in ref. [61] has an expected single clock stability of 3.1×10^{-18} at 1 s and will reach a sensitivity of 10^{-18} in 9 s. The QPN limit of the Th^{3+} trapped ion nuclear clock with 1 s probe time and a single ion is 8×10^{-17} at 1 s, reaching 10^{-18} at 1.7 h; using 10 ions (see ref. [60]) reduces it to 1 h. A solid-state nuclear clock will use the macroscopic number of Th ions embedded in a crystal and is expected to have much better stability. Moreover, 1,000-ion trapped ion clocks with a Coulomb crystal have already been proposed with a projected stability of 4.4×10^{-18} at 1 s (ref. [62]), reaching 10^{-18} in 19 s. The molecular and molecular ion clock stabilities are expected to follow those of the lattice neutral atom clocks and trapped ion clocks, respectively, as these are defined by the same type of operation parameters. At 10^{-13} eV, the DM effective coherence $\tau_\star$ is a few hours, which is still longer than it will take the clocks to reach the sensitivity floor. We note that DM sensitivity can be further improved by measurement over multiple coherence volumes[63].

The range of DM masses for which the DM frequency signal can be extracted without sensitivity loss depends on the parameters of the clock operation T_m and τ and the DM coherence time[64]. Generally, one needs to have at least one DM oscillation during the total measurement time τ, losing sensitivity beyond this point. For high frequencies, one eventually will have multiple DM oscillations during the free-precession (probe) time T_m, leading to a loss of sensitivity. This is particularly notable for this proposal, as the characteristic probe time of $T_m = 1$ s corresponds to a DM mass of 4×10^{-15} eV. This problem can be remedied for mass ranges of interest to the proposed mission by either reducing T_m (enabled by the excellent recent stability noted above) or applying an additional 'dynamical decoupling' (DD) series of π laser pulses during the clock probe time[22].

The DD scheme allows the coherent addition of the DM signal contribution over the probe time and, therefore, the extraction of the DM signal that oscillates on a faster timescale than the clock measurement cycle. The DD sequence can be optimized to probe the 10^{-13} eV mass range of specific interest to this work. Full numerical simulation of DM detection protocols with clocks with various dynamic decoupling sequences has been performed[63]. A simulation of various dynamic decoupling sequences, which includes quantum projection noise, laser noise and DM decoherence, demonstrated a clock sensitivity reach at all DM masses needed for this mission[63]. We also note that with the excellent stability of modern clocks discussed below, one can use a shorter probe time on the scale of 0.1 s and still achieve a design sensitivity well within the relevant DM coherence time.

Generally, clock probes are not continuous with some 20–50% of 'dead time' used for system cooling and so on. While a zero-dead-time clock has been demonstrated with two atomic ensembles[65], it is not required for our proposal owing to the high stability of modern clocks on the relevant timescales discussed above.

In summary, a wide variety of clocks can be selected for a pair of colocated mission clocks. An attractive possibility is to use Yb^+, which has two clock transitions in the same ion giving $\Delta K = 7$ (ref. [54]; the probe sequence will alternate between two transitions). Such a scheme removes uncertainty due to the gravitational potential and temperature differences between clock locations. The development of a two-transition Yb lattice clock as proposed in ref. [55] would have the same benefits and provide high stability enabled by thousands of trapped neutral atoms combined with a high sensitivity of $\Delta K = 15$. Comparing an Sr clock[66] to an ultrastable cavity[24] ($\Delta K = 1$) would utilize extraordinary clock stability but increasing cavity performance will require a cryogenic setup. Future development of a high-precision nuclear clock will enable an ultimate experiment with the highest potential discovery reach.

Data availability

The data that support the plots within this paper and other findings of this study are available from the corresponding author upon reasonable request.

Code availability

The code that generated the plots within this paper and other findings of this study are available from the corresponding author upon reasonable request.

References

1. Graham, P. W., Kaplan, D. E. & Rajendran, S. Cosmological relaxation of the electroweak scale. *Phys. Rev. Lett.* **115**, 221801 (2015).
2. Banerjee, A., Kim, H. & Perez, G. Coherent relaxion dark matter. *Phys. Rev. D* **100**, 115026 (2019).
3. Svrcek, P. & Witten, E. Axions in string theory. *J. High Energy Phys.* **06**, 051 (2006).
4. Peccei, R. D., Sola, J. & Wetterich, C. Adjusting the cosmological constant dynamically: cosmons and a new force weaker than gravity. *Phys. Lett. B* **195**, 183–190 (1987).
5. Hu, W., Barkana, R. & Gruzinov, A. Cold and fuzzy dark matter. *Phys. Rev. Lett.* **85**, 1158–1161 (2000).
6. Ely, T. A., Burt, E. A., Prestage, J. D., Seubert, J. M. & Tjoelker, R. L. Using the deep space atomic clock for navigation and science. *IEEE Trans. Ultrason. Ferroelectr. Freq. Control* **65**, 950–961 (2018).

7. Puetzfeld, D. & Lämmerzahl, C. (eds) *Relativistic Geodesy* Vol. 196 (Springer, 2019).
8. Gozzard, D. R. et al. Ultrastable free-space laser links for a global network of optical atomic clocks. *Phys. Rev. Lett.* **128**, 020801 (2022).
9. Yin, J. et al. Satellite-based entanglement distribution over 1200 kilometers. *Science* **356**, 1140 (2017).
10. Burt, E. et al. Demonstration of a trapped-ion atomic clock in space. *Nature* **595**, 43–47 (2021).
11. Liu, L. et al. In-orbit operation of an atomic clock based on laser-cooled ^{87}Rb atoms. *Nat. Commun.* **9**, 2760 (2018).
12. Arvanitaki, A., Huang, J. & Van Tilburg, K. Searching for dilaton dark matter with atomic clocks. *Phys. Rev. D* **91**, 015015 (2015).
13. Van Tilburg, K., Leefer, N., Bougas, L. & Budker, D. Search for ultralight scalar dark matter with atomic spectroscopy. *Phys. Rev. Lett.* **115**, 011802 (2015).
14. Banerjee, A., Budker, D., Eby, J., Kim, H. & Perez, G. Relaxion stars and their detection via atomic physics. *Commun. Phys.* **3**, 1 (2020).
15. Flacke, T., Frugiuele, C., Fuchs, E., Gupta, R. S. & Perez, G. Phenomenology of relaxion-Higgs mixing. *J. High Energy Phys.* **06**, 050 (2017).
16. Craig, N. Naturalness: a snowmass white paper. In *2022 Snowmass Summer Study*. Preprint at https://arxiv.org/abs/2205.05708 (2022).
17. Banerjee, A., Kim, H., Matsedonskyi, O., Perez, G. & Safronova, M. S. Probing the relaxed relaxion at the luminosity and precision frontiers. *J. High Energy Phys.* **07**, 153 (2020).
18. Maleki, L. & Prestage, J. SpaceTime Mission: clock test of relativity at four solar radii. In *Gyros, Clocks, Interferometers…: Testing Relativistic Graviy in Space* (Eds Lämmerzahl, C.) 369–380 (Springer, 2001).
19. Damour, T. & Donoghue, J. F. Phenomenology of the equivalence principle with light scalars. *Class. Quant. Grav.* **27**, 202001 (2010).
20. Hees, A., Guéna, J., Abgrall, M., Bize, S. & Wolf, P. Searching for an oscillating massive scalar field as a dark matter candidate using atomic hyperfine frequency comparisons. *Phys. Rev. Lett.* **117**, 061301 (2016).
21. Wcislo, P. et al. New bounds on dark matter coupling from a global network of optical atomic clocks. *Sci. Adv.* **4**, eaau4869 (2018).
22. Aharony, S. et al. Constraining rapidly oscillating scalar dark matter using dynamic decoupling. *Phys. Rev. D* **103**, 075017 (2021).
23. Antypas, D. et al. Scalar dark matter in the radio-frequency band: atomic-spectroscopy search results. *Phys. Rev. Lett.* **123**, 141102 (2019).
24. Kennedy, C. J. et al. Precision metrology meets cosmology: improved constraints on ultralight dark matter from atom-cavity frequency comparisons. *Phys. Rev. Lett.* **125**, 201302 (2020).
25. Oswald, R. et al. Search for oscillations of fundamental constants using molecular spectroscopy. *Phys. Rev. Lett.* **129**, 031302 (2022)
26. Bergé, J. et al. MICROSCOPE Mission: first constraints on the violation of the weak equivalence principle by a light scalar dilaton. *Phys. Rev. Lett.* **120**, 141101 (2018).
27. Wagner, T. A., Schlamminger, S., Gundlach, J. H. & Adelberger, E. G. Torsion-balance tests of the weak equivalence principle. *Class. Quant. Grav.* **29**, 184002 (2012).
28. Hees, A., Minazzoli, O., Savalle, E., Stadnik, Y. V. & Wolf, P. Violation of the equivalence principle from light scalar dark matter. *Phys. Rev. D* **98**, 064051 (2018).
29. Tsai, Y.-D., Wu, Y., Vagnozzi, S. & Visinelli, L. Asteroid astrometry as a fifth-force and ultralight dark sector probe. Preprint at https://arxiv.org/abs/2107.04038 (2021).
30. Veltmaat, J., Schwabe, B. & Niemeyer, J. C. Baryon-driven growth of solitonic cores in fuzzy dark matter halos. *Phys. Rev. D* **101**, 083518 (2020).
31. Anderson, N. B., Partenheimer, A. & Wiser, T. D. Direct detection signatures of a primordial Solar dark matter halo. Preprint at https://arxiv.org/abs/2007.11016 (2020).
32. Kaup, D. J. Klein-Gordon Geon. *Phys. Rev.* **172**, 1331–1342 (1968).
33. Pitjev, N. P. & Pitjeva, E. V. Constraints on dark matter in the solar system. *Astron. Lett.* **39**, 141–149 (2013).
34. Stadnik, Y. V. & Flambaum, V. V. Enhanced effects of variation of the fundamental constants in laser interferometers and application to dark-matter detection. *Phys. Rev. A* **93**, 063630 (2016).
35. Ludlow, A. D., Boyd, M. M., Ye, J., Peik, E. & Schmidt, P. O. Optical atomic clocks. *Rev. Mod. Phys.* **87**, 637–701 (2015).
36. Antypas, D. et al. New horizons: scalar and vector ultralight dark matter. Preprint at https://arxiv.org/abs/2203.14915 (2022).
37. Safronova, M. S. et al. Search for new physics with atoms and molecules. *Rev. Mod. Phys.* **90**, 025008 (2018).
38. Kozlov, M. G., Safronova, M. S., Crespo López-Urrutia, J. R. & Schmidt, P. O. Highly charged ions: optical clocks and applications in fundamental physics. *Rev. Mod. Phys.* **90**, 045005 (2018).
39. Peik, E. et al. Nuclear clocks for testing fundamental physics. *Quantum Sci. Technol.* **6**, 034002 (2021).
40. Kasper, J. C. et al. Parker solar probe enters the magnetically dominated solar corona. *Phys. Rev. Lett.* **127**, 255101 (2021).
41. Cavanaugh, J. F. et al. The mercury laser altimeter instrument for the MESSENGER Mission. *Space Sci. Rev.* **131**, 451–479 (2007).
42. Brewer, S. M. et al. $^{27}Al^{+}$ quantum-logic clock with a systematic uncertainty below 10^{-18}. *Phys. Rev. Lett.* **123**, 033201 (2019).
43. Sanner, C. et al. Optical clock comparison for Lorentz symmetry testing. *Nature* **567**, 204–208 (2019).
44. Bothwell, T. et al. JILA SrI optical lattice clock with uncertainty of 2.0×10^{-18}. *Metrologia* **56**, 065004 (2019).
45. Hanneke, D., Kuzhan, B. & Lunstad, A. Optical clocks based on molecular vibrations as probes of variation of the proton-to-electron mass ratio. *Quantum Sci. Technol.* **6**, 014005 (2021).
46. Lange, R. et al. Improved limits for violations of local position invariance from atomic clock comparisons. *Phys. Rev. Lett.* **126**, 011102 (2021).
47. Leefer, N., Gerhardus, A., Budker, D., Flambaum, V. V. & Stadnik, Y. V. Search for the effect of massive bodies on atomic spectra and constraints on yukawa-type interactions of scalar particles. *Phys. Rev. Lett.* **117**, 271601 (2016).
48. Derevianko, A. & Pospelov, M. Hunting for topological dark matter with atomic clocks. *Nature Phys.* **10**, 933 (2014).
49. Dailey, C. et al. Quantum sensor networks as exotic field telescopes for multi-messenger astronomy. *Nature Astron.* **5**, 150–158 (2021).
50. Stadnik, Y. V. Comment on "Quantum sensor networks as exotic field telescopes for multi-messenger astronomy". Preprint at https://arxiv.org/abs/2111.14351 (2021).
51. Derevianko, A. et al. Fundamental physics with a state-of-the-art optical clock in space. *Quantum Sci. Technol.* **7**, 044002 (2022).
52. Banerjee, A. et al. Searching for Earth/Solar axion halos. *J. High Energy Phys.* **09**, 004 (2020).
53. Flambaum, V. V. & Dzuba, V. A. Search for variation of the fundamental constants in atomic, molecular, and nuclear spectra. *Can. J. Phys.* **87**, 25–33 (2009).
54. Lange, R. et al. Improved limits for violations of local position invariance from atomic clock comparisons. *Phys. Rev. Lett.* **126**, 011102 (2021).

55. Safronova, M. S., Porsev, S. G., Sanner, C. & Ye, J. Two clock transitions in neutral Yb for the highest sensitivity to variations of the fine-structure constant. *Phys. Rev. Lett.* **120**, 173001 (2018).
56. Fadeev, P., Berengut, J. C. & Flambaum, V. V. Sensitivity of ^{229}Th nuclear clock transition to variation of the fine-structure constant. *Phys. Rev. A* https://doi.org/10.1103/PhysRevA.102.052833 (2020).
57. Flambaum, V. V. Enhanced effect of temporal variation of the fine structure constant and the strong interaction in Th229. *Phys. Rev. Lett.* **97**, 092502 (2006).
58. Weyers, S. et al. Advances in the accuracy, stability, and reliability of the PTB primary fountain clocks. *Metrologia* **55**, 789–805 (2018).
59. Stuhler, J. et al. Opticlock: transportable and easy-to-operate optical single-ion clock. *Measurement: Sensors* **18**, 100264 (2021).
60. Keller, J., Partner, H. L., Burgermeister, T. & Mehlstäubler, T. E. Precise determination of micromotion for trapped-ion optical clocks. *J. Appl. Phys.* **118**, 104501 (2015).
61. Bothwell, T. et al. Resolving the gravitational redshift within a millimeter atomic sample. *Nature* **602**, 420–424 (2022).
62. Leibrandt, D. R., Porsev, S. G., Cheung, C. & Safronova, M. S. Prospects of a thousand-ion Sn^{2+} Coulomb-crystal clock with sub-10^{-19} inaccuracy. Preprint at https://arxiv.org/abs/2205.15484 (2022).
63. Zaheer, M. H., Leibrandt, D., Hume, D. & Safronova, M. S. Quantum metrology algorithms for dark matter searches with ^{229} Th^{3+}. In *53rd Annual Meeting of the APS Division of Atomic, Molecular and Optical Physics* **67**, abstr. K05.00005 (2022).
64. Centers, G. P. et al. Stochastic fluctuations of bosonic dark matter. *Nat. Commun.* **12**, 7321 (2021).
65. Schioppo, M. et al. Ultrastable optical clock with two cold-atom ensembles. *Nat. Photon.* **11**, 48–52 (2016).
66. Bothwell, T. et al. Resolving the gravitational redshift within a millimeter atomic sample. *Nature* **602**, 420–424 (2022).
67. Vermeulen, S. M. et al. Direct limits for scalar field dark matter from a gravitational-wave detector. *Nature* **600**, 424–428 (2021).

Acknowledgements

We thank K. Abazajian, A. Cooray, C. Chen, J. Feng, M. Kaplinghat, H. Kim, D. Leibrandt, G. Perez, S. Profumo and T. Tait for useful discussions. We also thank A. Case and P. Whittlesey for the detailed discussions of instrumentation and environments in space missions, especially the solar probes. We thank D. Budker, Y. Stadnik, P. Thirolf and N. Yu for comments on the manuscript. The work of Y.-D.T. is supported in part by NSF Grant PHY-2210283 and in part by Simons Foundation Grant No. 623683. Part of this document was prepared by Y.-D.T. using the resources of the Fermi National Accelerator Laboratory (Fermilab), a US Department of Energy, Office of Science, HEP User Facility. Fermilab is managed by Fermi Research Alliance, LLC (FRA), acting under contract No. DE-AC02-07CH11359. The work of J. E. was supported by the World Premier International Research Center Initiative (WPI), MEXT, Japan, and by the Japanese Society for the Promotion of Science KAKENHI grant Nos. 21H05451 and 21K20366. This work is supported in part by US NSF grants Nos. PHY-2012068 and OMA-2016244. This work is a part of the 'Thorium Nuclear Clock' project that has received funding from the European Research Council (ERC) under the European Union's Horizon 2020 research and innovation programme (grant agreement No. 856415). Part of this work was performed at the Aspen Center for Physics, which is supported by the National Science Foundation grant no. PHY-1607611. We also thank the Simons Foundation for its generous support. J. E. thanks the Galileo Galilei Institute for Theoretical Physics for hospitality and the Istituto Nazionale Fisica Nuclear for partial support during the completion of this work.

Author contributions

All authors contributed to the writing and reviewing of the manuscript. Y.-D.T. conceived the preliminary ideas, initiated the DM study and studied further applications of space quantum clocks (including the spatial variation of fundamental constants and future applications) while cross-checking all results. J.E. analysed the properties of SHs and produced the final figures used in the manuscript. M.S.S. provided expertise on clock technologies and related sensitivity estimates.

Competing interests

The authors declare no competing interests.

Additional information

Supplementary information The online version contains supplementary material available at https://doi.org/10.1038/s41550-022-01833-6.

Correspondence and requests for materials should be addressed to Yu-Dai Tsai, Joshua Eby or Marianna S. Safronova.

Peer review information *Nature Astronomy* thanks the anonymous reviewers for their contribution to the peer review of this work